Electrical transport in Na, K, Rb, and Cs fullerides: Phase formation, microstructure, and metallicity

F. Stepniak, P. J. Benning, D. M. Poirier, and J. H. Weaver
Department of Materials Science and Chemical Engineering, University of Minnesota, Minneapolis, Minnesota 55455
(Received 21 December 1992)

The electrical properties of the alkali-metal fullerides have been investigated via parallel resistivity measurements and photoelectron spectroscopy. Phase formation associated with the incorporation of Na, K, Rb, and Cs into C_{60} films is reflected by the dependence of resistivity on temperature and alkali-metal concentration. Photoemission spectra show the details of the filling of states derived from the lowest unoccupied molecular level and the consequences of electron correlation. For K-C_{60} and Rb-C_{60} films, the resistivity and photoemission results indicate metallic character only for the A_3C_{60} phase. Changes in the temperature coefficient of resistivity for Rb-C_{60} as a function of doping reveal the granular nature of the film and show the transition from insulating to metallic character. In contrast, the Na and Cs fullerides are insulators for all concentrations. The temperature-dependent resistivity results for Na_xC_{60} show a phase transformation at 226 K for x between two and three, but neither phase is metallic.

INTRODUCTION

Investigations of the alkali-metal fullerides A_xC_{60} have raised questions concerning the development of discrete phases and their metallic or insulating character, particularly for thin films. To date, there have been very few studies of electrical transport of the fullerides in the normal state that could reveal the relationship between phase formation, electronic structure, and electron transport. Kochanski *et al.*[1] have discussed resistivity measurements of K_xC_{60} films with ~ 60 Å grains that demonstrate that the minimum in $\rho(x)$ occurs at $x=3\pm0.05$ and that potassium saturation occurs at $x=6$. Xiang *et al.*[2] have reported temperature-dependent resistivity results for single-crystal K_3C_{60} that show that the $x=3$ phase behaves like an ordinary metal.

In this paper, we discuss resistivity and photoemission measurements of the Na, K, Rb, and Cs fullerides made from films of C_{60} exposed to increasing amounts of alkali metals. Differences in behavior across the alkali-metal-fulleride family reflect phase formation and the importance of electron correlation in determining the electrical properties near the metal-insulator transition. Valence-band photoemission results demonstrate the transfer of charge from the alkali-metal atom to fill states derived from the lowest unoccupied molecular orbital (LUMO) of C_{60}. Analysis of core-level photoemission spectra, detailed in Ref. 3, indicates phase separation with preferential occupation of interstitial sites based on the size of the alkali-metal ion. Resistivity results presented here affirm the growth of discrete phases in A_xC_{60} films and they show how these phases influence electron transport. The temperature dependence of the resistivity establishes that the Na and Cs fullerides are insulating at all concentrations. In contrast, K_xC_{60} and Rb_xC_{60} show metallic behavior near $x=3$, and the change in resistivity as a function of stoichiometry and temperature can be effectively described within the framework of granular metal theory, i.e., the nucleation and growth of a metallic phase in an insulating medium. The very low conductivities of the metallic phases are consistent with significant electron-electron repulsion effects.

EXPERIMENT

Resistivity and photoemission measurements were performed on films grown on sapphire substrates. The resistivities of fulleride films were determined using the method of Van der Pauw. For electrical contact, triangular pads were formed on the corners of the 1-cm^2 sapphire wafers by successively evaporating 1000 Å of Ti and Ag. Subsequently, copper wires were attached to the pads with silver epoxy. The temperature dependence of the resistivity, $\rho(T)$, was measured from 45 to 425 K. The temperature was determined using a Au-Fe/Chromel thermocouple in intimate contact with the sample holder. A filament adjacent to the holder was used for heating. Cooling was provided via a closed cycle He refrigerator.

Purified C_{60} was evaporated from Ta boats located 8 cm from the sapphire substrate. The amount deposited was monitored with a quartz-crystal thickness monitor. The alkali metals were sublimed from well-degassed SAES getter sources arranged in a similar geometry. Chamber pressures were maintained below 2×10^{-9} Torr while depositing C_{60} and below 3×10^{-10} Torr during alkali-metal deposition. The substrates were held at 300 K during film growth. Post-growth annealing was done at 425 K for ~ 10 min.

High-resolution photoemission valence-band spectra were obtained in a chamber equipped with a He lamp as well as an Al K_α x-ray source. Photoemitted electrons were collected with a double-pass cylindrical mirror analyzer. The resolution (electrons plus photons) was 160 meV for the He lamp results. The total resolution, including the thermal broadening of the Fermi function, was 195 meV. Concurrently, films were grown on a

0163-1829/93/48(3)/1899(8)/$06.00

grounded Pt foil to assess charging related to photoemission. Such effects were negligible except when the measurements were done at low temperature or at ultralow dopant concentrations.

ELECTRICAL TRANSPORT

Concentration-dependent resistivities

It is now well known that photoemission and inverse photoemission processes produce final states with energy-level spectra for pure C_{60} that are shifted from the ground state because of electron-electron correlation.[4] Good agreement between theory and experiment can be obtained by aligning the bands derived from the highest occupied molecular orbitals (HOMO) for the occupied states. Alignment of the LUMO-derived band shows good agreement for the unoccupied states.[5] These electric states are delocalized on the scale of the molecule, yet localized on the scale of nearest neighbors so that narrow bands are produced. Electron energy-loss measurements[6] and optical-absorption measurements[7] show an onset near 1.5 eV, but extrapolation of the HOMO and LUMO bands measured by photoemission and inverse photoemission[4,8] gives a band gap of 2.6 eV (the band-center-to-band-center energy is 3.7 eV). The apparent discrepancy can be understood by noting that the lowest-energy optical absorption creates an electron-hole pair localized on an individual molecule, i.e., a Frenkel exciton, whereas the ionizing processes of photoemission and inverse photoemission create separated $N-1$ and $N+1$ states. The energy difference between the separated and unseparated configurations is a measure of the correlation energy, ~ 2 eV.[4,9] As far as transport properties are concerned, the energy required to generate intrinsic separated charge carriers is the true band gap. C_{60} films show slightly enhanced conductivity when exposed to photons of energy ~ 1 eV less than the band gap.[10,11] This reflects the generation of free carriers via the interaction of excitons with defects or surfaces, an effect that is well known for polynuclear aromatic molecular crystals.[12]

Measurements of electrical transport in pure C_{60} are difficult because of its high intrinsic resistivity and the sensitivity to light exposure and trace impurities that introduce band-gap states.[13] Studies of the photoinduced xerographic discharge[10] in mixtures of C_{60} and C_{70} and studies of the resistivity of pure C_{60} at high pressures[14] suggest electronic transport via localized states. In fact, transport of charge carriers in all the insulating fullerides can be thought of in terms of hopping between negatively charged C_{60} molecules where the overlap of molecular orbitals is small. Electron localization is less severe in the metallic fullerides and transport is dominated by multiple scattering events, as will be discussed below. We can make reliable resistivity measurements only when $\rho < 500$ Ω cm, a condition that is reached by doping when the overall stoichiometry is A_xC_{60}, $x \cong 0.1$. We note that the resistivity of oxygen-free C_{60} films has been reported to be 10^8 Ω cm (Ref. 15) while films composed of mixtures of C_{60} and C_{70} exposed to air have a resistivity near 10^{14} Ω cm.[16]

Starting from pure face-centered-cubic[17] (fcc) C_{60}, x-ray diffraction studies[18–25] have reported K_3C_{60} and Rb_3C_{60} phases where the C_{60} lattice remains fcc and the alkali-metal ions occupy octahedral and tetrahedral interstitial sites. K-, Rb-, and Cs-C_{60} form a body-centered tetragonal A_4C_{60} phase, and further doping results in a saturated body-centered-cubic (bcc) A_6C_{60} phase. Also identified have been Na_2C_{60}, Na_3C_{60}, and Na_6C_{60} phases where the C_{60} lattice remains fcc. From valence-band and core-level photoemission analysis, the fcc phases of these fullerides (except for Na_3C_{60}) have been identified in our thin films samples.[3,26] Core-level studies show that the fcc octahedral and tetrahedral sites provide bonding configurations for the K, Rb, and Cs ions that are spectroscopically distinguishable. By this method, Poirier *et al.*[3] have reported that Rb and Cs fill only octahedral interstitials at low concentration giving an A_1C_{60} phase (NaCl structure). The chemical environment is very similar in the tetrahedral interstitial sites of the A_4C_{60} and A_6C_{60} phases and the A_4C_{60} phase cannot be unambiguously isolated by core-level fitting. Recently the valence-band signatures of K_4C_{60} have been identified.[27] Photoemission spectra[3,13,26] show nearly identical C 1*s* core-level and valence-band behavior for the saturated phases, regardless of whether the phases are derived from bcc, (K, Rb, Cs) or fcc (Na) structures. Hence the features in the electronic structure at $x=6$ are molecular in nature and are derived from the C_{60} orbitals. (This is in contrast to what is observed for the alkaline earth fullerides where hybridization is important.[28]) The goal of the present study was to measure the resistivity $\rho(x,T)$ of fulleride films so that the transport properties could be correlated with structural and electronic properties for all values of x and temperatures between 45 and 425 K.

Figure 1 summarizes resistivity results obtained during alkali-metal incorporation in 500–4000-Å C_{60} films. The symbols indicate points at which exposure to the alkali-metal source was interrupted, the sample annealed, and photoemission spectra taken to determine the x value. The solid lines drawn through the measured points of Fig. 1 approximate the resistivity behavior during the exposure between annealing cycles. The stoichiometries were deduced from the carbon and alkali-metal core-level intensities and the relative intensity of the LUMO-derived feature. As a reference point, it was assumed that the saturated phase was A_6C_{60}. The estimated uncertainty is $x=\pm 0.2$. Four-point probe measurements were monitored continuously during alkali-metal exposure. Current/voltage readings exhibited a $\sim 5\%$ drift over a few minutes when exposure was interrupted at 300 K. Smaller variations were induced by annealing at 425 K for 10 min. Thereafter, the magnitudes of $\rho(x)$ at room temperature were unchanged. This is consistent with facile diffusion of alkali-metal ions and the formation of film microstructures that were stable against mild annealing. All the films in this study were at least 500 Å thick to avoid the thickness dependence of $\rho(x)$ reported by Kochanski *et al.*[1] for K_3C_{60} films.

Each curve of Fig. 1 shows a rapid decrease in resistivity upon doping to $x \sim 0.5$, then a slower decrease to a

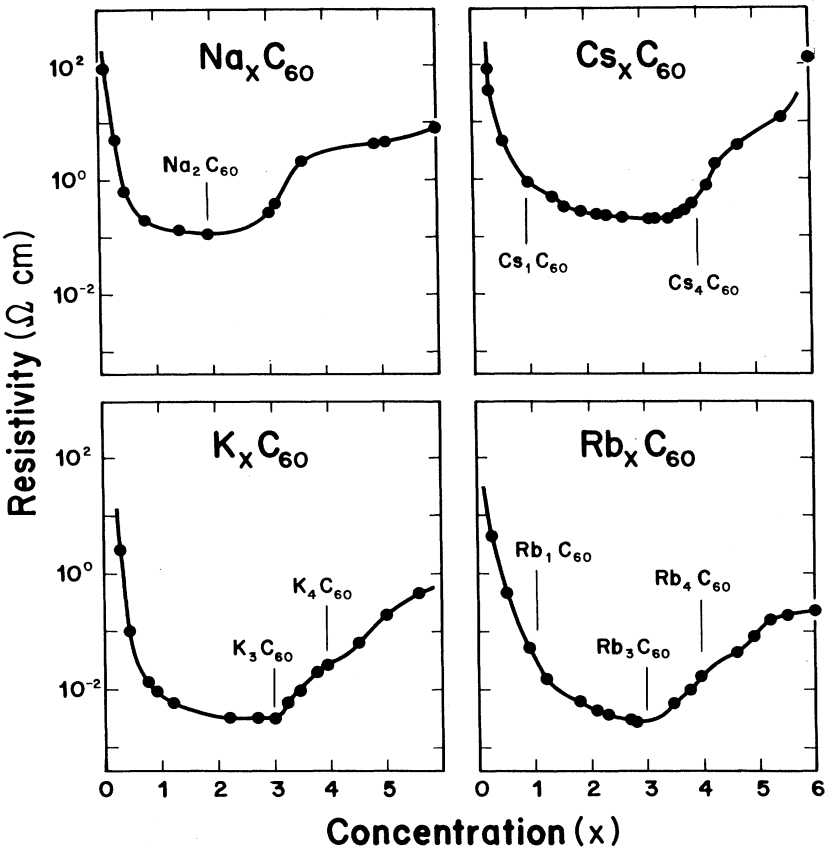

FIG. 1. $\rho(x)$ for thick films of C_{60} doped with Na, K, Rb, and Cs. Points indicate where exposure to the alkali-metal source was stopped and x-ray and ultraviolet photoemission spectra were acquired to determine concentration. The labels indicate the known fulleride phases at 300 K. The minima in $\rho(x)$ occur for stoichiometries corresponding to Na_2C_{60}, K_3C_{60}, Rb_3C_{60}, and $Cs_{3.5}C_{60}$. Structure in $\rho(x)$ can be associated with the development of the different phases.

minimum between $x=2$ and 3.5 before increasing to a maximum at $x=6$. The minimum resistivity values occur at different stoichiometries for the different fullerides. The minimum resistivity values were very close to those reported by Haddon *et al.*,[29] namely 0.11 Ω cm for Na-C_{60}, 0.0031 Ω cm for K-C_{60}, 0.028 Ω cm for Rb-C_{60}, and 0.20 Ω cm for Cs-C_{60}. At the minimum resistivity for each fulleride, the resistivity was measured as a function of temperature to determine the temperature coefficient of resistance (TCR). In this way, the metallic or insulating character of the film could be determined since metals become better conductors at lower temperatures (TCR > 0) while insulators show better conductivities at higher temperatures (TCR < 0). We found that Na- and Cs-C_{60} are insulators even at their minimum resistivity. In contrast, K- and Rb-C_{60} show metallic behavior for x near 3. Note that the $\rho(x)$ curves of Fig. 1 show structures that are due to phase formation, features not previously observed.[29]

The labels in Fig. 1 draw attention to the stoichiometries of the fulleride phases at 300 K. Stoichiometries away from the indicated phases produce samples containing a mixture of two phases, even for equilibrium growth. This is a consequence of the Gibbs phase rule. Thus the deposition of alkali-metal atoms onto a C_{60} film will initially yield a solid solution or α phase, but doping beyond the solubility limit results in the nucleation of fulleride grains in the solution phase matrix. The first fulleride phase is $x=1$ for Cs and Rb, $x=2$ for Na, and $x=3$ for K. The size of these grains will depend on the interfacial free energy and kinetics of growth. It is important to recognize that doping under conditions that prevent equilibrium phase formation can introduce additional phases that coexist with the first two. Such nonequilibrium growth has been discussed for K_xC_{60} in detail elsewhere[27,30] where it was shown that the K_4C_{60} phase appears during vapor-phase deposition before completion of the $x=3$ phase. To fully understand the electrical properties of fulleride films, we must determine the properties of each phase and examine effects related to the microstructure.

Figure 1 shows that the resistivities of Na_xC_{60}, K_xC_{60}, and Rb_xC_{60} films are similar for $x<0.5$ even though Na prefers tetrahedral sites,[25] Rb prefers octahedral sites,[3] and K ions occupy both sites.[22] The differences in $\rho(x)$ for $x>0.5$ undoubtedly reflect the fact that the films are derived from disparate equilibrium phases. The stoichiometries of the first line phases imply differences in the relative amounts of the fulleride phases for a given x value and, probably, the microstructure in this two-phase regime. The presence of a Rb_1C_{60} phase but not a K_1C_{60} phase is clearly seen in the $\rho(x)$ behavior near $x=1$ where there is a larger resistivity and shoulder in $\rho(x)$ for Rb_1C_{60}. Hence a film with $x=1$ for Rb_xC_{60} will be predominantly nonmetallic Rb_1C_{60} whereas a K_xC_{60} film with $x=1$ will be α-C_{60}(K) plus metallic K_3C_{60}. Na_2C_{60}

is nonmetallic and the film resistances are larger than for the Rb- and K-C_{60} films, though $\rho(x)$ for $0<x<2$ falls intermediately between the Rb_xC_{60} and K_xC_{60} curves. Figure 1 also shows that the resistivity of Cs_xC_{60} is much higher than the other fullerides for the α phase and in the region where there is phase separation into α-C_{60}(Cs) and Cs_1C_{60}. This may well be a consequence of the Cs ions in octahedral sites producing a lattice expansion that reduces the intermolecular wave-function overlap relative to the smaller Rb ions in the corresponding sites of Rb_1C_{60}.

The minimum resistivity values occur at stoichiometries when the films are derived almost entirely from a single phase, near Na_2C_{60}, K_3C_{60}, Rb_3C_{60}, and Ca_4C_{60}, corresponding to stable phases near half-band filling. As mentioned above, K_3C_{60} and Rb_3C_{60} are metallic and Na_2C_{60} and Cs_4C_{60} are insulators. For Na, there has been a report[25] that Na_3C_{60} forms at elevated temperature but disproportionates into fcc-based Na_2C_{60} and fcc-based Na_6C_{60} at low temperature. From the resistivity results of Fig. 1, we find that $\rho(x)$ has started to increase by $x=3$ at 300 K. This indicates that whatever coexists with Na_2C_{60} for x near 3 has a higher resistivity and cannot be metallic. Qualitatively, a model assuming only ideal Na_2C_{60} and Na_6C_{60} phases for Na_xC_{60} cannot reproduce the observed shoulder in $\rho(x)$ at $x\sim3.5$. It is plausible that the shoulder about halfway between 2 and 6 is a consequence of disorder in the alkali-ion distribution. Such disorder would affect the hopping integrals that describe transport in these molecular crystals. This disorder could be the result of a solid solution phase between $x=2$ and 6. Unfortunately, a detailed description of octahedral site filling for $2<x<6$ in Na_xC_{60} to determine whether there is phase separation or solid solution behavior must await analytical refinement of x-ray diffraction results.[25]

For the fullerides of K, Rb, and Cs, x-ray diffraction analysis[21–24] has shown the formation of the A_4C_{60} body-centered tetragonal structure. The $\rho(x)$ results for K_xC_{60} and Rb_xC_{60} show a shoulder at $x=4$, indicating that the A_4C_{60} phases have resistivities intermediate to those of the A_3C_{60} and A_6C_{60} phases. The A_4C_{60} compounds are nonmetallic, as demonstrated by a negative TCR and the lack of photoemission intensity at the Fermi level.[27,30] Cs_xC_{60} consistently maintains a higher resistivity than K- and Rb-C_{60} and there is a very broad resistivity minimum at $x\cong3.5$ before completion of the Cs_4C_{60} phase.

The resistivity results for each alkali-metal fulleride show an increase as x approaches 6. Photoemission valence-band spectra[13,26] for the A_6C_{60} phases of Na, K, Rb, and Cs show complete filling of the sixfold-degenerate LUMO band and a shift of the LUMO band away from E_F, i.e., when there are no holes in the LUMO states to pin E_F. The resistivities of K_6C_{60} and Rb_6C_{60} are substantially lower than Cs_6C_{60} (Fig. 1), again presumably because the alkali-ion-induced lattice dilation for K and Rb is smaller. For Cs_xC_{60}, we speculate that there is a high tolerance to Cs vacancies for the Cs_4C_{60} and Cs_6C_{60} phases, consistent with the fact that the Cs_6C_{60} phase is more difficult to prepare and less stable to annealing *in vacuo* than the other saturated alkali-metal fullerides. Thus the amount of disorder would be large for x near 4 and 6 and electrical transport would be hindered. For Na_6C_{60}, there are four Na ions in the octahedral site of the fcc structure and one in each tetrahedral site[25] so direct comparison is not possible. Finally, comparison shows that the resistivities for the A_6C_{60} phases are much lower than for pure C_{60}. While both C_{60} and A_6C_{60} are closed-shell molecular crystals, the transport gaps for the A_6C_{60} structures are smaller than for pure C_{60}.[13]

Granular metal transport in K and Rb fullerides

Interest in the K and Rb fullerides has been particularly strong because their A_3C_{60} phases are metals[29] and exhibit superconductivity.[20,31,32] Here we focus on the Rb_xC_{60} system since it forms a nonmetallic Rb_1C_{60} phase, in addition to the metallic Rb_3C_{60} phase, and the effects of the transition from the $x=1$ to the $x=3$ phase can be readily seen in the temperature-dependent transport properties. In the discussion below, we compare our results to those predicted based on a granular metal model, i.e., a model for the effective resistivity of a solid derived from phase-separated grains of metallic and nonmetallic constituents.

Transport properties for composites of immiscible metal and insulator phases, known as granular metal films,[33] exhibit three distinct behaviors, termed metallic, transitional, and dielectric, according to the volume ratio of the metal and insulator grains. At high metal concentrations, isolated particles of the insulator are dispersed in a metallic continuum. At low metal concentration the roles of the two species are reversed as the insulator makes up the continuum and the metallic grains are isolated. A maze or labyrinth structure of interconnected metal and insulator particles marks the transition between the metallic and dielectric regions at intermediate metal concentrations. The overall electrical properties of granular metal films depend critically on these concentration-dependent structures. Films in the metallic region behave like common metals with the stipulation that transport is dominated by electron scattering effects due to grain boundaries. In the dielectric region, electrons can move only by tunneling between isolated metallic grains. In the transition region, transport of charge carriers is derived from both tunneling and electron percolation through interconnected grains. Each structural region, shown schematically in the insets of Fig. 2, is characterized by the sign of TCR.

Figure 2 shows a logarithmic plot of $\rho(T)$ versus $T^{-1/2}$ for Rb_xC_{60} with x values that correspond to volume ratios of Rb_3C_{60} to Rb_1C_{60} of 0.20 ($x=1.4$), 0.55 ($x=2.1$), and 0.90 ($x=2.8$). The insets represent the general microstructure in each region. Figure 2 shows that the TCR is negative in the dielectric region, $x=1.4$, then goes to zero in the transition region, $x=2.1$, and is positive in the metallic region, $x=2.8$.

The dielectric region of a granular metal film is charac-

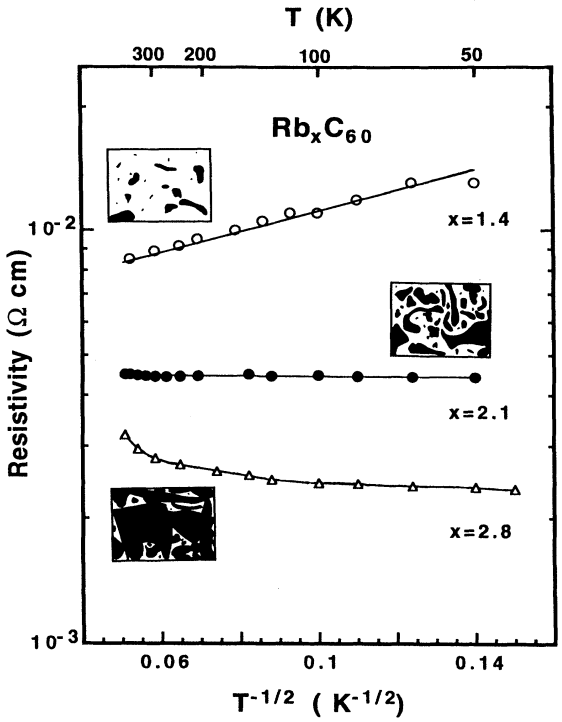

FIG. 2. $\rho(T)$ for Rb_xC_{60} with $x=1.4$, 2.1, and 2.8 plotted vs $T^{-1/2}$. These films are composed of metallic Rb_3C_{60} grains in a matrix of insulating Rb_1C_{60}, i.e., a granular metal as depicted in the insets. The linear behavior for $x=1.4$ is indicative of transport via tunneling between isolated metallic grains of variable size (dielectric regime with insulator dominating). The resistivity is independent of temperature at $x=2.1$, characteristic of a transition between insulator and metallic behavior when tunneling and electron percolation contribute equally to conduction. At $x=2.8$, the film exhibits true metallic behavior and the resistivity lies just below the Mott limit.

terized by a negative TCR because charge transfer can occur only by tunneling between isolated metal grains. Charge transfer between two neutral grains produces neighbors of positive and negative charge. Hence there is a charging energy that is dependent on the grain size, grain separation, and the dielectric strength of the insulator. In the limit of small electric fields, tunneling is thermally activated and described by Boltzmann statistics. Sheng, Abeles, and Arie[34] have derived an expression where the logarithm of the resistivity was proportional to $T^{-1/2}$ for a film in the dielectric region, assuming a distribution of grain sizes for the metallic component. Since the nucleation and growth of Rb_3C_{60} grains in the Rb_1C_{60} matrix should produce random grain sizes, we compare our results to this model. From Fig. 2, it is clear that $\rho(T)$ for $x=1.4$ shows the characteristic $T^{-1/2}$ behavior, confirming the applicability of the model. Significantly, comparison of the behavior for $x=1.4$ to that for granular metal films consisting of Ni-SiO_2, Al-Al_2O_3 or Au-Al_2O_3 (Ref. 35) shows nearly identical temperature dependence in the dielectric region for this same volume fraction of the metal phase, ~ 0.2.

The TCR decreases as x increases from 1.4 to 2.1 and $\rho(T)$ retains its linear dependence on $T^{-1/2}$. This decrease in the TCR is expected because the spacing between metal grains decreases. As metal grains fuse, a random network of metallic channels allows electron percolation to contribute to the conductivity, supplementing the tunneling process. The TCR goes to zero when the conductivity of the film is determined equally from continuous metal networks and tunneling, as shown for $x=2.1$ in Fig. 2. The resistivity at this point is 4.5×10^{-3} Ω cm, a value very close to the Mott limit,[36] i.e., 5×10^{-3} Ω cm. This value is consistently seen in granular metal systems with similar metal-to-insulator volume ratios. For conventional granular metals (e.g., Au in Al_2O_3, Ni in SiO_2), however, $\rho(x)$ shows a greater decrease with concentration in this transition region. This can be understood by noting that the insulating Rb_1C_{60} phase has a relatively low resistivity ($\rho=35\times10^{-3}$ Ω cm) and the metallic Rb_3C_{60} phase has a high resistivity compared to metal-insulator films such as Ni-SiO_2.

The small but positive TCR for $Rb_{2.8}C_{60}$ is characteristic of a granular film in the metallic regime. The rate of decrease in the TCR slows with cooling but remains positive to 45 K. Our results for $Rb_{2.8}C_{60}$ and $K_{2.7}C_{60}$ (not shown) are equivalent to those reported for single crystal K_3C_{60} (Ref. 2) even though the samples studied here, grown on sapphire, are certainly polycrystalline and composed of small, randomly oriented grains. Other reports for thin film samples of K-C_{60} have shown insulatorlike behavior upon cooling (TCR <0 for $T<200$ K).[37] We speculate that the nonmetallic TCR behavior observed previously reflects the presence of impurities, not the polycrystalline nature of the film as previously suggested. Small amounts of oxygen, for example, would have a profound effect on the fulleride film makeup. While the grain size does not change the sign of the TCR, grain size is more important for characterization of the superconducting properties of the fullerides. In particular, the width of the transition temperature at T_c is much sharper for films having grains larger than the superconducting coherence length of 100 Å.[2,37]

Modification of the electrical transport properties of granular metals due to grain boundary scattering has been studied extensively.[33] In composites where the metal volume fraction dominates, the average metallic grain size can be modified by annealing. Samples consisting of large metallic grains exhibit a slow decrease in resistivity with increasing metal concentration since insulator particles offer a small scattering surface area. Electron scattering is much more effective in small-grained granular films since charge carriers must follow a tortuous path. Figure 1 shows that the resistivity changes gradually with concentration for Rb_xC_{60} as x approaches 3, acting like a large-grained material. Hence electron scattering involving Rb_3C_{60} grain boundaries is not significant. Indeed, nearly identical resistivities of large and small grained samples of K_3C_{60} (Refs. 1 and 2) indicate that the resistivity is independent of grain size.

The effective electron scattering length λ influences the magnitude of the resistivity. A simple treatment of transport using the Boltzmann equation gives a value of λ on the order of a single C_{60} molecule, a scattering length

that is small even for 100-Å grains. While this very small λ could reflect orientational disorder that is present in the crystal,[38] a more likely explanation is that the short electron scattering length reflects correlation in this doped molecular solid. Moreover, the wide LUMO-derived feature and low conductivity of Rb_3C_{60} suggest that conduction electron states are still somewhat localized, as discussed previously based on photoemissions results for K_3C_{60}.[27] While phonon-electron interactions could also provide a mechanism for localization, this effect must be small because the magnitude of the spectral weight shift observed in LUMO can only be explained by electron-electron effects.

We emphasize that only the A_3C_{60} phases of K and Rb are metallic, and thus these phases can be the only singularly alkali-metal-doped superconducting fullerides. Indeed, Rb or K doping beyond $x=3$ resulted in a second transition between the metallic 3-phase and the insulating 4-phase. The $\rho(T)$ results for $Rb_{3.3}C_{60}$ are identical to those for $Rb_{2.1}C_{60}$ where TCR=0. The TCR became negative with further Rb incorporation and the $T^{-1/2}$ dependence on $\rho(T)$ was recovered.

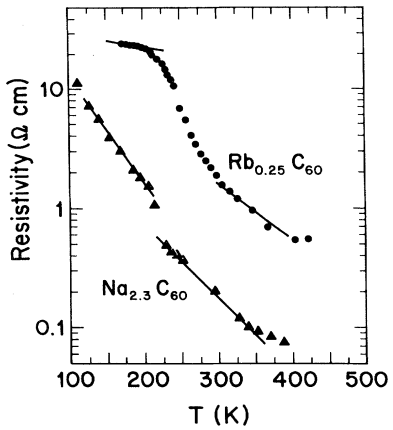

FIG. 3. $\rho(T)$ for $Na_{2.3}C_{60}$ and $Rb_{0.25}C_{60}$ showing negative temperature coefficients of resistance as is characteristic of insulators. For $Rb_{0.25}C_{60}$, the broad transition in $\rho(T)$ reflects the reduction in rotational motion and enhanced ordering at low temperature, i.e., the temperature-dependent effective overlap of the fullerene charge distribution. For $Na_{2.3}C_{60}$, the discontinuity in $\rho(T)$ at 226 K reflects a reversible phase transformation.

Temperature-dependent phase transformations

Changes in the resistivity with temperature for a fixed concentration make it possible to detect phase transformations, complementing such techniques as differential scanning calorimetry. Since each phase has a characteristic resistance and, for nonmetallic phases, a characteristic activation energy, the resistance should change discontinuously and the slope of $\rho(T)$ should change at a phase transition.

For pure C_{60}, there is a well-known phase transition at 249 K due to a conversion from the fcc to the simple cubic (sc) structure.[39] This reflects an optimization of the molecular orientations with the bonds of the high π electron density of one molecule arranged in areas of low electron density of adjacent molecules. While the high resistance of pure C_{60} makes it impossible for us to observe this ordering transition, we felt that suitable alkali-metal doping might enable such measurements. To our knowledge, the fcc-sc transition has not been observed previously in alkali-metal-doped C_{60}. From simple steric considerations, the occupation of tetrahedral sites should more severely inhibit the simple cubic optimization, so we judged Rb doping with octahedral site occupancy to offer a better chance of observing the ordering transition. Hence we investigated $Rb_{0.25}C_{60}$, where the microstructure reflects the presence of the Rb_1C_{60} phase with complete octahedral site occupancy and the α-C_{60}(Rb) phase with preferred filling of the octahedral interstitials.

Figure 3 shows that $\rho(T)$ for $Rb_{0.25}C_{60}$ is nearly constant from 170 to 210 K but then drops rapidly until flattening out at $\sim$360 K. The rate of change is largest between 240 and 275 K. The transition occurs between the room-temperature value where the molecules are spinning isotropically and the low-temperature value where the molecules are essentially fixed but merohedrally disordered.[17,38,39] The slopes of the lines drawn for $T>290$ K and $T<210$ K give the TCR in the low- and high-temperature regimes. Since the wave-function overlap between nearest-neighbor C_{60} molecules should vary with rotational orientation, the hopping probability of charge carriers will change and this will in turn affect the resistivity. Thus the broad transition region reflects the decrease in the rate of molecular rotation with decreasing temperature. The broad transition is consistent with NMR measurements[40] that have shown a widening of the characteristic ^{13}C spectral line over a 100-K region as the molecular rotation is reduced. The width of our transition may be exaggerated since the solubility limit of the α phase should be temperature dependent. Note, however, that changes in content in the α phase should not add features to the resistivity curve beyond broadening the background.

The report of an fcc Na_3C_{60} phase,[25] along with the absence of superconductivity in Na-C_{60} and a resistivity minimum at $x=2$, motivated us to examine $\rho(x,T)$ for Na_xC_{60} for $2\leq x\leq 3$. Figure 3 shows that $\rho(T)$ for $Na_{2.3}C_{60}$ exhibits a jump near 225 K and a change in the TCR. This behavior indicates an ordering transition that we have not observed for $x<2$ or $x>3$. While there is still uncertainty in the distribution of Na ions in the octahedral site for $2\leq x\leq 6$, the present results and those of Ref. 25 suggest further study would be fruitful. At the same time, neither the transport nor the photoemission results indicate metallic character at any temperature for Na_xC_{60} for x near 3.

Electronic structure

The above discussion has emphasized the stoichiometry- and temperature-dependent electrical behavior of the alkali-metal-fulleride films. Parallel photoemission spectra were acquired to correlate the resistivity measurements with changes in occupation of the

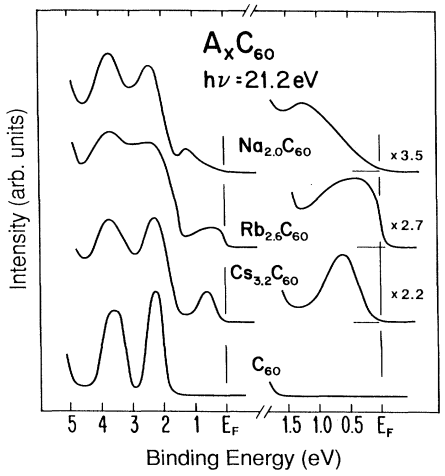

FIG. 4. Representative valence-band spectra of A_xC_{60} taken in parallel with the resistivity measurements. All of the spectra are normalized to height, not to concentration. The leading two features for pure C_{60} are derived from molecular π states. Alkali-metal incorporation draws the molecular LUMO-derived band below E_F. $Rb_{2.6}C_{60}$ exhibits metallic character because of its dominant Rb_3C_{60} content. The spectra of $Cs_{3.2}C_{60}$ and Na_2C_{60} show that both fullerides are insulators.

LUMO-derived band. Figure 4 shows photoemission spectra from the two leading bands of C_{60} and the occupancy of the LUMO band for representative fullerides. The photoemission results agree with the resistivity results, showing no emission at E_F for the nonmetallic Na and Cs fullerides and substantial emission for metallic Rb_xC_{60}. The 10–90 % width of the Fermi-level cutoff is 195 meV at 300 K. The curves are normalized to constant height to emphasize line-shape features and peak positions relative to E_F. Curves on the right are scaled by the figure indicated relative to those on the left.

It has been shown previously that the C_{60} valence bands extend $\sim$20 eV below E_F with narrow-band structures that are characteristic of a highly symmetric molecule in a van der Waals solid.[41] The leading two features, HOMO and HOMO-1, are centered 2.3 and 3.7 eV below E_F in pure C_{60}. Their relative intensities depend on the photon energy due to matrix element effects,[42] and these effects must be taken into account when determining x values from valence-band emission.

$Rb_{2.6}C_{60}$ exhibits a distinct Fermi-level cutoff together with a broadening of spectral features derived from HOMO and HOMO-1. For a film with this stoichiometry, we expect a mixture of the Rb_1C_{60} and Rb_3C_{60} phases so that the broadening reflects the overlap of emission from the two places. Analogous broadening has been observed for K-C_{60} and the contributions from the constituent species have been identified.[27] For both, the metallic Fermi edge reflects the metallic resistivity; we find no evidence of a pseudogap.[43] As for K-C_{60}, the width of the LUMO-derived band is inconsistent with band-structure calculations and reflects electron-electron correlation in the metallic phase.[44]

The top curve of Fig. 4 was obtained for Na-C_{60}, corresponding to the stoichiometry having the minimum resistivity. Na_2C_{60} is characterized by a LUMO-derived peak that is 1.1 eV from the HOMO band, compared to 1.6 eV for the metallic fullerides, and the absence of emission at E_F. With increasing doping, a new feature developed $\sim$0.5 eV below E_F, without overlapping E_F, and the film resistivity increased. Gu *et al.*[26] have argued that the different fullerides fall on opposite sides of a metal-insulator transition mediated by electron-electron repulsion. For Na-C_{60}, correlation effects produce a gap between upper and lower Hubbard-like bands and insulatorlike transport properties.

Figure 4 also shows the valence-band spectra of $Cs_{3.2}C_{60}$. This composition was chosen intermediate between the resistivity minima at $x=3$ for K and Rb fullerides and $x=3.5$ for Cs_xC_{60}. While emission at E_F diminishes in K- and Rb_xC_{60} for $3>x>4$, no states are observed at E_F for Cs_xC_{60} in this concentration range. In fact, the LUMO-derived feature for $Cs_{3.2}C_{60}$ is very similar in shape and position to those observed for the isostructural A_4C_{60} phases of K and Rb,[13,26] centered 0.6 eV below E_F. The absence of emission at E_F is consistent with the much larger resistivity of Cs-C_{60} compared to K-C_{60} or Rb-C_{60} for a comparable stoichiometry. Again, band theory would predict the Cs_4C_{60} phase to be metallic but electron correlation induces a band splitting. These results indicate that the composite film is derived from a mixture of insulating Cs phases.

CONCLUSION

Electrical transport in the normal state for the alkali-metal fullerides reflects the growth of discrete phases and the importance of correlation in these doped molecular crystals. The TCR results show that only the K_3C_{60} and Rb_3C_{60} phases are metallic and they have conductivities that are consistent with highly correlated metals. Rb_xC_{60} undergoes an insulator-metal-insulator transition as x increases from 1 to 4 and the $\rho(x,T)$ results are well described in the framework of granular metal theory.

ACKNOWLEDGMENTS

This work was supported by the National Science Foundation and Office of Naval Research. We thank R. E. Smalley, L. P. F. Chibante, T. Ohno, and Y. Chen for their contributions to this work.

[1]G. P. Kochanski, A. F. Hebard, R. C. Haddon, A. T. Fiory, Science **255**, 184 (1992).

[2]X.-D. Xiang, J. G. Hou, G. Briceno, W. A. Vareka, R. Mostovoy, A. Zettl, V. H. Creipi, and M. L. Cohen, Science **256**, 1190 (1992).

[3]D. M. Poirier, T. R. Ohno, G. H. Kroll, P. J. Benning, F. Stepniak, J. H. Weaver, L. P. F. Chibante, and R. E. Smalley, Phys. Rev. B **47**, 9870 (1993).

[4]J. H. Weaver, J. Phys. Chem. Solids **53**, 1433 (1992).
[5]J. L. Martins, N. Troullier, and J. H. Weaver, Chem. Phys. Lett. **180**, 457 (1991).
[6]E. Sohmen, J. Fink, R. H. Baughman, and W. Krätschmer, Z. Phys. B **86**, 87 (1992).
[7]A. Skumanich, Chem. Phys. Lett. **182**, 486 (1991); S. L. Ren *et al.*, Appl. Phys. Lett. **59**, 2678 (1991).
[8]M. B. Jost, P. J. Benning, D. M. Poirier, J. H. Weaver, L. P. F. Chibante, and R. E. Smalley, Chem. Phys. Lett. **184**, 423 (1991).
[9]R. W. Lof, M. A. van Veenendaal, B. Koopmans, H. T. Jonkman, and G. A. Sawatzky, Phys. Rev. Lett. **68**, 3924 (1992).
[10]J. Mort, M. Machonkin, R. Ziolo, D. R. Huffman, and M. I. Ferguson, Appl. Phys. Lett. **60**, 1735 (1992); J. Mort, M. Machonkin, R. Ziolo, and I. Chen, *ibid.* **61**, 1829 (1992).
[11]H. Yonehara and C. Pac, Appl. Phys. Lett. **61**, 575 (1992).
[12]J. I. Katz, S. A. Rice, S. Choi, and J. Jortner, J. Chem. Phys. **39**, 1683 (1963).
[13]P. J. Benning, D. M. Poirier, T. R. Ohno, Y. Chen, M. B. Jost, F. Stepniak, G. H. Kroll, J. H. Weaver, J. Fure, and R. E. Smalley, Phys. Rev. B **45**, 6899 (1992).
[14]N. Núñez Regueiro, P. Manceau, A. Rassat, P. Bernier, and A. Zehab, Nature **354**, 289 (1991).
[15]T. Arai, Y. Murakami, H. Suematsu, K. Kikuchi, Y. Achiba, and I. Ikemoto, Solid State Commun. **84**, 827 (1992).
[16]J. Mort, R. Ziolo, M. Machonkin, D. R. Huffman, and M. I. Ferguson, Chem. Phys. Lett. **186**, 284 (1991).
[17]R. M. Fleming, T. Siegrist, P. M. Marsh, B. Hessen, A. R. Kortan, D. W. Murphy, R. C. Haddon, R. Tycko, G. Dabbagh, A. M. Mujsce, M. L. Kaplan, and S. M. Zahurak, in *Clusters and Cluster-Assembled Materials,* edited by R. S. Averback, J. Bernholc, and D. L. Nelson, MRS Symposia Proceedings No. 206 (Materials Research Society, Pittsburgh, 1991), p. 691.
[18]P. W. Stephens, L. Mihaly, P. L. Lee, R. L. Whetten, S.-M. Huang, R. Kaner, F. Diederich, and K. Holczer, Nature **351**, 632 (1991).
[19]O. Zhou, J. E. Fischer, N. Coustel, S. Kycia, Q. Zhu, A. R. McGhie, W. J. Romanow, J. P. McCauley, Jr., A. B. Smith III, and D. E. Cox, Nature **351**, 462 (1991).
[20]K. Holczer, O. Klein, S.-M. Huang, R. B. Kaner, K.-J. Fu, R. L. Whetten, and F. Diederich, Science **252**, 1154 (1991).
[21]R. M. Fleming, M. J. Rosseinsky, A. P. Ramirez, D. W. Murphy, J. C. Tully, R. C. Haddon, T. Siegrist, R. Tycko, S. H. Glarum, P. Marsh, G. Dabbagh, S. M. Zahurak, A. V. Makhija, and C. Hampton, Nature **352**, 701 (1991).
[22]Q. Zhu, O. Zhou, N. Coustel, G. B. Vaughan, J. P. McCauley, Jr., W. J. Romanow, J. E. Fischer, and A. B. Smith III, Science **254**, 545 (1991).
[23]P. W. Stephens, L. Mihaly, J. B. Wiley, S.-M. Huang, R. B. Kaner, F. Diederich, R. L. Whetten, and K. Holczer, Phys. Rev. B **45**, 453 (1992).
[24]E. Y. Murakami, T. Arai, H. Suematsu, K. Kikuchi, N. Nakahara, Y. Achiba, and I. Ikemote, Mater. Sci. Eng. (to be published).
[25]M. J. Rosseinsky, D. W. Murphy, R. M. Fleming, R. Tycko, A. P. Ramirez, T. Siegrist, G. Dabbagh, and S. E. Barrett, Nature **356**, 416 (1992); T. Yildirim, O. Zhou, J. E. Fischer, N. Bykovetz, R. A. Strongin, M. A. Cichy, A. B. Smith III, C. L. Lin, and R. Jelinek, *ibid.* **360**, 566 (1992).
[26]C. Gu, F. Stepniak, D. M. Poirier, M. B. Jost, P. J. Benning, Y. Chen, T. R. Ohno, J. L. Martins, J. H. Weaver, J. Fure, and R. E. Smalley, Phys. Rev. B **45**, 6348 (1992).
[27]P. J. Benning, F. Stepniak, D. M. Poirier, J. L. Martins, J. H. Weaver, L. P. F. Chibante, and R. E. Smalley, Phys. Rev. B **47**, 13 843 (1993).
[28]Y. Chen, D. M. Poirier, M. B. Jost, C. Gu, T. R. Ohno, J. L. Martins, J. H. Weaver, L. P. F. Chibante, and R. E. Smalley, Phys. Rev. B **46**, 7961 (1992); Y. Chen, F. Stepniak, J. H. Weaver, L. P. F. Chibante, and R. E. Smalley, *ibid.* **45**, 8845 (1992).
[29]R. C. Haddon, A. F. Hebard, M. J. Rosseinsky, D. W. Murphy, S. J. Duclos, K. B. Lyons, B. Miller, J. M. Rosamilia, R. M. Fleming, A. R. Kortan, S. H. Glarum, A. V. Makhiga, A. J. Muller, R. H. Eick, S. M. Zahurak, R. Tycko, G. Dabbagh, and F. A. Theil, Nature **350**, 320 (1991).
[30]J. H. Weaver, P. J. Benning, F. Stepniak, and D. M. Poirier, J. Phys. Chem. Solids **53**, 1707 (1992).
[31]A. F. Hebard, M. J. Rosseinsky, R. C. Haddon, D. W. Murphy, S. H. Glarum, T. T. M. Palstra, A. P. Ramirez, and A. R. Kortan, Nature **350**, 600 (1991).
[32]M. J. Rosseinsky, A. P. Ramirez, S. H. Glarum, D. W. Murphy, R. C. Haddon, A. F. Hebard, T. T. M. Palstra, A. R. Kortan, S. M. Zahurak, and A. V. Makhija, Phys. Rev. Lett. **66**, 2830 (1991).
[33]B. Abeles, *Granular Metal Films, Applied Solid State Science* (Academic, New York, 1976), Vol. 6, p. 1, and references therein; J. E. Morris, A. Mello, and C. J. Adkins, in *Physical Phenomena in Granular Materials,* edited by T. H. Geballe, D. Sheng, and G. D. Cody, MRS Symposia Proceedings No. 195 (Materials Research Society, Pittsburgh, 1990), p. 181.
[34]P. Sheng, B. Abeles, and Y. Arie, Phys. Rev. Lett. **31**, 44 (1973).
[35]J. J. Hauser, Phys. Rev. B **7**, 4099 (1973); B. Abeles, P. Sheng, M. D. Coutts, and Y. Arie, Adv. Phys. **24**, 407 (1975).
[36]N. F. Mott, Adv. Phys. **16**, 49 (1967).
[37]T. T. M. Palstra, R. C. Haddon, A. F. Hebard, and J. Zaanen, Phys. Rev. Lett. **68**, 1054 (1992).
[38]M. P. Gelfand and J. P. Lu, Phys. Rev. Lett. **68**, 1050 (1992).
[39]P. A. Heiney, J. E. Fischer, A. R. McGhie, W. J. Romanow, A. M. Denenstein, J. P. McCauley, Jr., and A. B. Smith III, Phys. Rev. Lett. **66**, 2911 (1991); W. I. F. David, R. M. Ibberson, J. C. Matthewman, K. Prassides, T. S. Dennis, J. P. Hare, H. W. Kroto, R. Tyler, and D. R. M. Walton, Nature **353**, 147 (1991).
[40]R. Tycko, R. C. Haddon, G. Dabbagh, S. H. Glarum, D. C. Douglass, and A. M. Mujsce, J. Phys. Chem. **95**, 518 (1991).
[41]D. L. Lichtenberger, K. W. Nebesny, C. D. Ray, D. R. Huffman, and L. D. Lamb, Chem. Phys. Lett. **176**, 203 (1991); D. L. Lichtenberger, M. E. Jatcko, K. W. Nebesny, C. D. Ray, D. R. Huffman, and L. D. Lamb, in *Electrical Transport in Na, K, Rb and Cs,* edited by R. S. Averback, J. Bernholc, and D. L. Nelson, MRS Symposia Proceedings No. 206 (Materials Research Society, Pittsburgh, 1991), p. 673; J. H. Weaver, J. L. Martins, T. Komeda, Y. Chen, T. R. Ohno, G. H. Kroll, N. Troullier, R. E. Haufler, and R. E. Smalley, Phys. Rev. Lett. **66**, 1741 (1991).
[42]P. J. Benning, D. M. Poirier, N. Troullier, J. L. Martins, J. H. Weaver, R. E. Haufler, L. P. F. Chibante, and R. E. Smalley, Phys. Rev. B **44**, 1962 (1991).
[43]T. Takahashi, S. Suzuki, T. Morikawa, H. Katayama-Yoshida, S. Hasegawa, H. Inokuchi, K. Seki, K. Kikuchi, S. Suzuki, K. Ikemoto, and Y. Achiba, Phys. Rev. Lett. **68**, 1232 (1992).
[44]P. J. Benning, F. Stepniak, and J. H. Weaver (unpublished).